Cell Death and Differentiation (2004) 11, 631–644

www.nature.com/cdd

DAP-kinase-mediated morphological changes are localization dependent and involve myosin-II phosphorylation

S Bialik[1], AR Bresnick[2] and A Kimchi*[,1]

[1] Department of Molecular Genetics, Weizmann Institute of Science, Rehovot, Israel;
[2] Department of Biochemistry, Albert Einstein College of Medicine, Bronx, NY, USA
* Corresponding author: A Kimchi, Department of Molecular Genetics, Weizmann Institute of Science, Rehovot 76100, Israel.
Tel: +972-8-934-2428; Fax: +972-8-931-5938;
E-mail: adi.kimchi@weizmann.ac.il

Received 16.6.03; revised 27.10.03; accepted 03.12.03; published online 27.2.04
Edited by Dr G Kroemer

Abstract

DAP-kinase (DAPk) is a Ser/Thr kinase that regulates cytoplasmic changes associated with programmed cell death. It is shown here that a GFP–DAPk fusion, which partially localized to actin stress fibers, induced extensive membrane protrusions. This phenotype correlated with changes in myosin-II distribution and with increased phosphorylation of the myosin-II regulatory light chain (RLC). A mutant lacking the cytoskeletal-interacting region (GFP–DAPkΔCyto) displayed diffuse cytoplasmic localization, and induced peripheral membrane blebbing, instead of the extensive protrusions. In contrast, deletion of the ankyrin repeats led to mislocalization of the kinase to focal contacts, where it failed to elicit any changes in cell morphology. While both wild-type DAPk and DAPkΔCyto induced RLC phosphorylation independently of the Rho-activated kinase ROCK, only the wild type led to increases in stress-fiber associated phospho-RLC. Thus, the precise intracellular localization of DAPk is critical for exposure to its substrates, including the RLC, which mediate varying morphologic changes.

Cell Death and Differentiation (2004) **11,** 631–644.
doi:10.1038/sj.cdd.4401386
Published online 27 February 2004

Keywords: DAP-kinase; myosin regulatory light chain; actin; membrane blebbing; contraction; apoptosis

Abbreviations: CaM, calmodulin; DAPk, DAP-kinase; MBS, myosin binding subunit; MLCK, myosin light chain kinase; RLC, myosin-II regulatory light chain

Introduction

DAP-kinase (DAPk) is a Ser/Thr Ca^{2+}-calmodulin (CaM)-regulated, death-associated kinase.[1] It is the prototype for a family of death-inducing kinases, which includes DRP-1 and ZIP-kinase (ZIPk).[2–6] In addition to the conserved catalytic module, DAPk harbors multiple functional domains, including eight ankyrin repeats, a cytoskeletal interacting region, and a C-terminal death domain.[1] DAPk activity is necessary for the induction of cell death by ceramide, matrix detachment, oncogene expression, TNF-α, Fas, TGF-β, and IFN-γ, and overexpression leads to pronounced death-associated cellular changes, which include membrane blebbing, cell rounding, and the formation of autophagic vesicles.[7–13] As a correlate of its death-promoting effects, DAPk acts as a tumor suppressor, functioning in a p53-mediated checkpoint that suppresses oncogene-induced cellular transformation and also acting as an antimetastasis factor.[8,9] Moreover, DAPk expression is lost in numerous malignant cell lines,[14] as well as in human tumor specimens such as cervical carcinoma, non-small-cell lung cancer, B-cell malignancies, and head and neck cancer.[15–19] In some cases, reduced expression levels have been correlated with metastatic progression, disease recurrence, and unfavorable prognosis.[18,20–22]

Despite its critical role as a tumor suppressor, little is known about the direct molecular mechanisms by which DAPk causes cell death. Catalytic activity is required for its death-inducing capabilities,[1] yet DAPk's *in vivo* substrates have not been identified. Previous studies have demonstrated that endogenous DAPk fractionates with insoluble, actin-dependent structures in HeLa cells, and that the cytoskeleton interacting region is critical for full DAPk activity *in vivo*.[1] DAPk's localization to specific regions of the cytoskeleton may bring it into close proximity with its physiological substrates. One potential cytoskeletal-associated substrate is the myosin-II regulatory light chain (RLC), previously shown to be phosphorylated *in vitro* by DAPk.[1] In nonmuscle and smooth muscle cells, phosphorylation of the 20 kDa RLC on Ser-19 activates myosin-II, promoting filament assembly, actin binding, and ultimately, acto-myosin contraction.[23] However, it is not known if the RLC is a DAPk substrate *in vivo*, and the significance of RLC phosphorylation in the kinase's overall death phenotype is unknown.

In this study, we examined the significance of DAPk's association with the cytoskeleton. Using a GFP fusion protein, we localized DAPk to actin filaments in HeLa cells and observed the changes in intracellular localization and cell morphology over time. We characterized two protein domains critical for localization and phenotypic outcome, and identified the RLC as an *in vivo* substrate that most likely mediates DAPk-induced contractions, protrusions, and membrane blebbing.

Results

DAPk localization to actin filaments requires the ankyrin repeats and the cytoskeletal interacting region

In order to assess the role of cytoskeletal localization in DAPk's function, a GFP–DAPk fusion protein was generated

and used to assess the precise localization of DAPk in viable cells, to track possible changes in localization over time, and to examine how localization influences its ability to mediate morphological events. The addition of GFP to the N-terminus of HA-tagged DAPk did not have any deleterious effect on its ability to induce the previously characterized morphologic changes in 293T cells or on its *in vitro* kinase activity (data not shown).

When expressed in HeLa cells with a well-developed cytoskeleton, GFP–DAPk formed linear arrays that extended to the edge of the cell and into large protrusions (Figure 1a). In addition, a more diffuse distribution was observed. The latter could represent a second subcellular localization of DAPk, or may result from the saturation of endogenous DAPk binding sites due to overexpression of the kinase. Costaining with phalloidin and analysis by confocal microscopy indicated that these linear arrays coincided with filamentous actin (Figure 1b). Colocalization was seen both in stress fibers as well as in cortical actin filaments (arrows in Figure 1b). Moreover, paxillin, a component of focal adhesions, localized

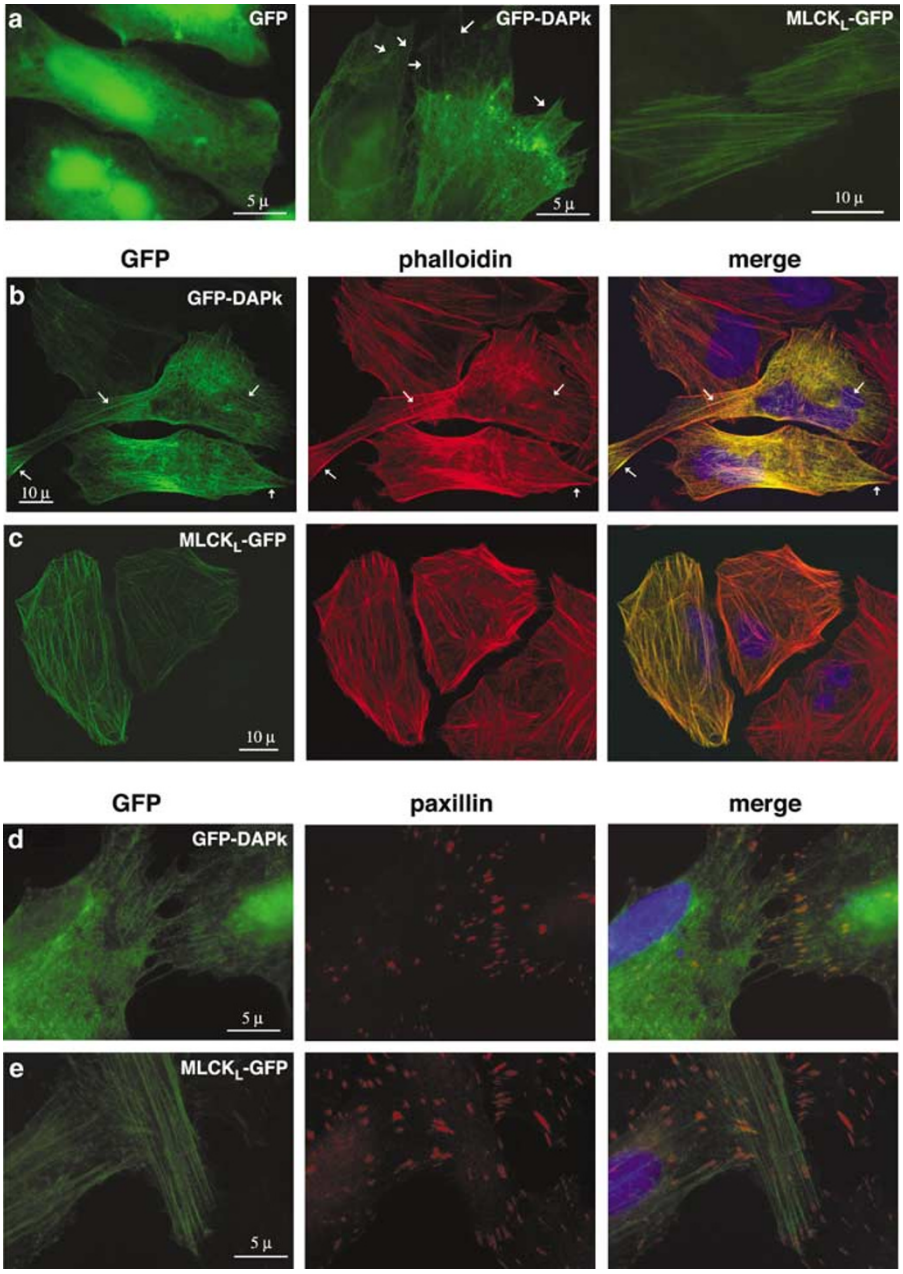

Figure 1 GFP–DAPk localizes to actin stress fibers. (**a**) HeLa cells expressing GFP (left panel), GFP–DAPk (middle panel) or MLCK$_L$–GFP (right panel). (**b**,**c**) GFP–DAPk (**b**)- or MLCK$_L$–GFP (**c**)-transfected cells were stained with Texas Red-conjugated phalloidin to visualize F-actin and viewed by confocal microscopy. Arrows in (**b**) indicate DAPk localization to actin stress fibers and cortical actin filaments. (**d–e**) GFP–DAPk (**d**)- or MLCK$_L$-GFP (**e**)-transfected cells were stained for paxillin to visualize focal contacts. The left and middle panels of (**b–e**) show the GFP and rhodamine/Texas Red channels, respectively, while the right panels represent digitally merged images, and include DAPI-stained nuclei

in close proximity to the tips of the DAPk filaments (Figure 1d), indicating that stress fibers containing DAPk extended to focal contacts. The DAPk/actin filaments were not well organized in the cell, but extended in various directions in an asymmetric pattern. Also, within a single cell, GFP–DAPk was not evenly distributed on the filaments, with some areas of individual stress fibers containing more DAPk than others (compare shades of yellow and orange of overlap in right panel of Figure 1b), and some fibers lacking visible GFP–DAPk. This contrasts with the previously described long myosin light chain kinase ($MLCK_L$–GFP) fusion,[24] which localizes to well-organized, thick filaments (e.g. Figure 1a) that coincide completely and uniformly with actin stress fibers (Figure 1c), extending to the focal contacts (Figure 1e). In fact, expression of MLCK results in increased fiber formation in these same cells (see also Poperechnaya *et al*.[24] and Blue *et al*.[25]). GFP alone, in contrast, exhibited a diffuse cytoplasmic localization with strong nuclear accumulation (Figure 1a), and showed no significant overlap with actin filaments (data not shown). Additional staining indicated that DAPk did not associate with microtubules, or cellular organelles such as ER, lysosomes, and autophagic vesicles (data not shown).

The localization of DAPk to filamentous structures depended on an intact actin cytoskeleton. Upon treatment of cells with the actin depolymerizing agent latrunculin B, the linear arrays disappeared and GFP–DAPk reorganized into aggregates throughout the cell (Figure 2a, panels d and e). Following the removal of latrunculin, DAPk was observed once again in filamentous structures, particularly at the cell periphery (e.g. Figure 2a panel f, arrows). Similar treatment with DMSO alone had no effect on the DAPk localization (Figure 2a, panels a–c). Significantly, costaining with phalloidin indicated that the latrunculin-induced DAPk aggregates colocalized with the reorganized F-actin (Figure 2b). Thus, DAPk is tightly associated with F-actin and its localization depends on actin organization.

Two deletion mutants, lacking functionally important subdomains of DAPk, were used to examine the contribution of these subdomains to DAPk's intracellular localization (Figure 3a). The first mutant, GFP–DAPkΔAnk, lacks the ankyrin repeats (residues 365–629), a protein–protein interaction domain prominent in cytoskeletal proteins. The second construct, GFP–DAPkΔCyto, lacks the cytoskeletal interacting region (residues 641–835), previously shown to mediate DAPk's resistance to detergent extraction.[1] As expected, GFP–DAPkΔCyto exhibited an exclusively diffuse cytoplasmic localization, confirming that the cytoskeletal interacting domain is critical for DAPk's association with actin filaments (Figure 3b). Surprisingly, GFP–DAPkΔAnk accumulated in linear, barb-like structures (Figure 3c), which exhibited colocalization with paxillin upon confocal microscopy analysis (Figure 3d). Thus, GFP–DAPkΔAnk predominantly localizes to focal contacts, although thin

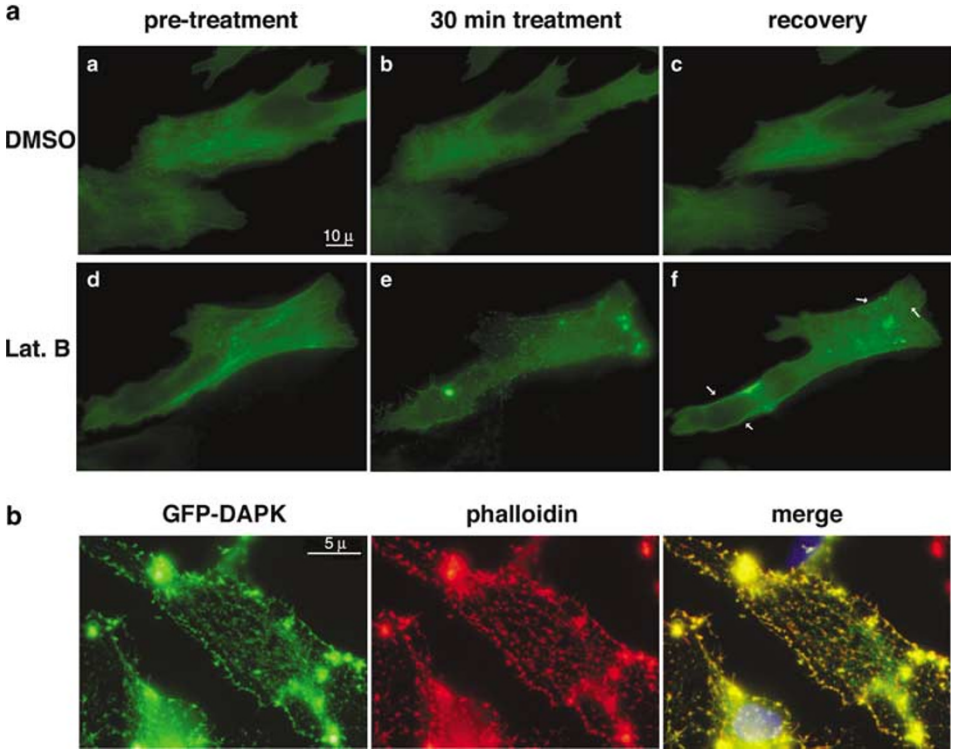

Figure 2 GFP–DAPk filament formation requires intact actin cytoskeleton. (**a**) HeLa cells grown on gridded coverslips were transfected with GFP–DAPk, treated with DMSO (a–c) or latrunculin B (d–f), and then allowed to recover in normal growth media. For each experimental condition, individual live cells were monitored prior to treatment (a, d), 30 min after treatment (b, e), and 30 min after recovery (c, f). Scale bar shown in panel (a) applies to all panels. Arrows in panel (f) indicate newly formed filaments. (**b**) Cells treated with latrunculin were fixed and stained with Texas Red-conjugated phalloidin to visualize F-actin. The right panel represents digitally merged images, and includes DAPI-stained nuclei

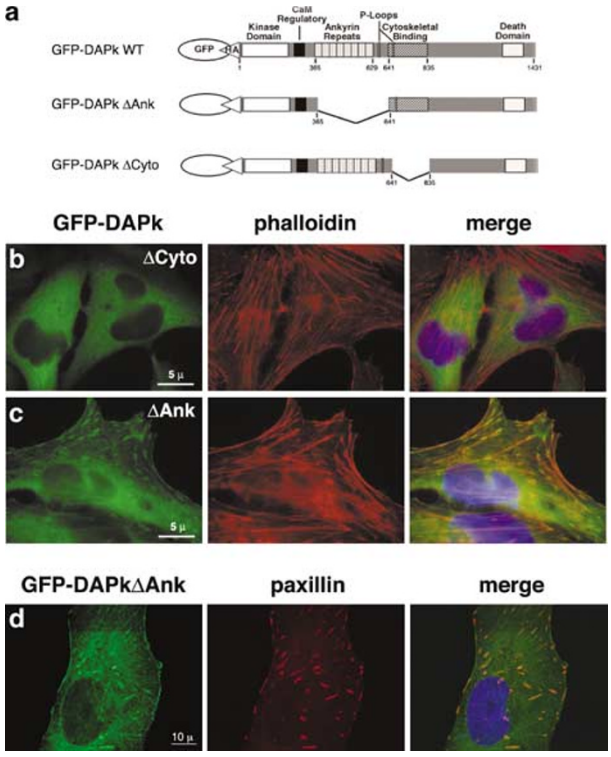

Figure 3 GFP–DAPk localization requires the cytoskeletal domain and the ankyrin repeats. (**a**) Diagram of GFP–DAPk WT and deletion mutants. (**b–d**) Intracellular localization of DAPk mutants. GFP–DAPkΔCyto (**b**)- and GFP–DAPkΔAnk (**c, d**)-transfected cells were stained with Texas Red-conjugated phalloidin to visualize F-actin (**b, c**) or were stained with an antibody to paxillin and rhodamine-conjugated secondary antibody (**d**) to visualize focal contacts. The cell shown in panel (**d**) was imaged by confocal microscopy. The right panels represent merged images of the GFP (left) and Texas Red/rhodamine (middle) channels, and include DAPI-stained nuclei

filaments were detected on occasion. These observations indicate that the ankyrin repeats are not required for DAPk's association with components of the cytoskeleton, but are involved in the alignment of DAPk along the actin filaments. Thus, both the cytoskeletal interacting region and the ankyrin repeats are critical for the proper localization of DAPk.

DAPk induces major changes in cell morphology, including cell protrusions and membrane blebbing

The use of a GFP–DAPk fusion allowed changes in cell morphology and DAPk localization to be observed in live cells. The majority of nontransfected or GFP-transfected cells exhibited a flat, adherent morphology (Figure 4e). In contrast, GFP–DAPk expression caused significant changes in cell morphology (Figure 4a,b). Many cells remained flat and adherent, but projected lamellipodia-like protrusions and extensions of the cell body, which gave them a larger, more spread appearance (phenotype 1, Figure 4a left panel). These extrusions, which were unique to DAPk-expressing cells, formed from all regions of the cell body. In these cells, GFP–DAPk was cytoplasmic, and was also aligned in linear structures, particularly in elongated portions of the cell (e.g. single arrows). GFP–DAPk also accumulated at the periphery of the protrusions (e.g. double arrows). Other cells appeared less spread, with protrusions that were no longer flat, but which were constricted and appeared to be retracting (phenotype 2, Figure 4a, middle panel). Often the nucleus was found within these protrusions (Figure 4a, middle panel and also Figures 5d and 6c). A third population of cells had rounded cell bodies with short protrusions that appeared as bulges of the cell periphery (phenoytpe 3, Figure 4a, right panel). These bulges were not round and symmetrical, but were elongated, and of varying sizes. GFP–DAPk-containing filaments were less apparent in the second and third populations; instead, the protein formed a bright ring along the edge of the protrusions and bulges (see double arrows, Figure 4a). The relative proportion of these phenotypes depended on the efficiency of transfection and the expression levels achieved. For example, in one representative experiment, 28% of cells exhibited a flat, spread morphology with extended protrusions (phenotype 1), while 59% were contracted with constricted protrusions and bulges (phenotypes 2, 3). The remaining transfected cells were morphologically indistinguishable from nontransfected cells. To evaluate if these different morphologies represent progressive stages leading to a terminal state, individual cells were repeatedly examined over time. Figure 4b shows a pair of cells observed over 6 h. At the start of observation, these particular cells were flat with some minor protrusions (Figure 4b, panel a). Over the next 3–4 h, the edges of the protrusions began to ruffle, and retract towards the cell body (Figure 4b, panels b–d), producing cells that resembled the second phenotype shown in the middle panel of Figure 4a. The cells continued to retract, forming rounded cell bodies surrounded by large protrusion-like structures (Figure 4b, panel e). After 6 h, an amorphous bulged structure remained (Figure 4b, panel f).

Localization of DAPk to stress fibers was essential for the full range of morphologic changes observed. GFP–DAPk-ΔAnk-expressing cells did not differ morphologically from those expressing GFP alone, and no obvious phenotypic changes were observed even after several hours of observation (Figure 4c, compare to 4e). Thus, when DAPk localizes to focal contacts, it cannot induce the morphological changes that are observed with the full-length, stress fiber-associated kinase. The expression of GFP–DAPkΔCyto also did not produce large protrusions and cell extensions, although it had severe effects on cell morphology. Depending on the transfection, approximately one-half to two-thirds of transfected cells appeared smaller than controls (e.g., Figure 4d, panel a), with condensed nuclei (data not shown). In addition, a subset of these cells exhibited peripheral membrane blebbing, which differed both in extent and appearance compared with the protrusions and bulges induced by the full-length DAPk (e.g., Figure 4d, panel b). In one representative experiment, 16.6% of GFP–DAPkΔCyto-transfected cells were small and round without blebs, while 42.9% were small and blebbed. Figure 4d shows the progression of these phenotypes. In panel a, small, blebless cells were observed. With time, small, spherical blebs formed from the cell surface (panel b). Each bleb extruded over a few seconds, at which

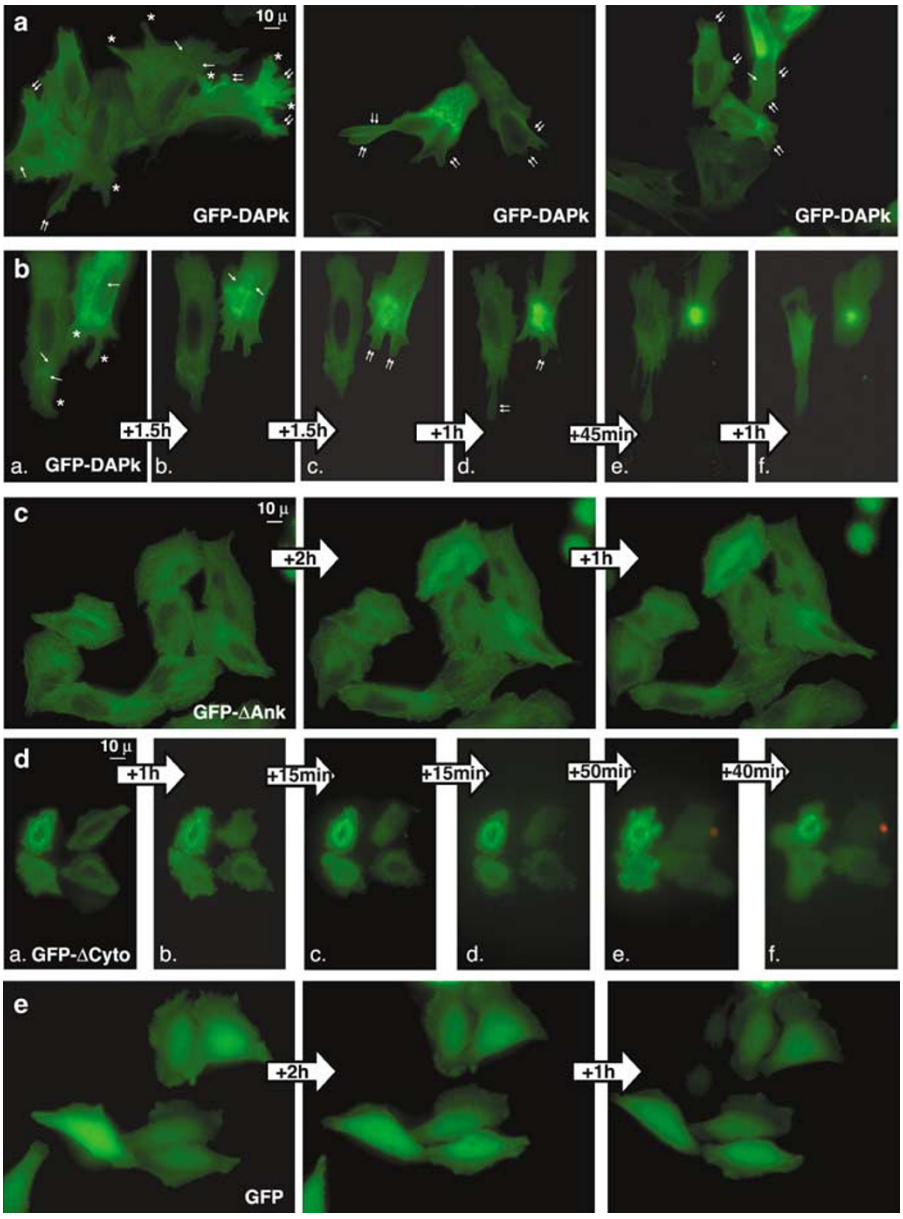

Figure 4 Changes in cell morphology and localization of GFP–DAPk constructs in live HeLa cells. HeLa cells were transfected with GFP–DAPk WT (**a, b**), GFP–DAPkΔAnk (**c**), GFP–DAPkΔCyto (**d**), or GFP alone (**e**) and observed 15–18 h later. For panels (**b–e**) the same group of cells was viewed periodically for up to 6 h, with the first panel corresponding to the start of observation. Block arrows between panels indicate the passage of time between observation points. Asterisks in (**a, b**) denote protrusions, while single arrows and double arrows indicate DAPk on filamentous arrays and lining ruffled cell protrusions, respectively. All panels are shown at the same magnification; scale bar is shown in panels (**a**), (**c**) and (**d**)

point it stopped growing, while other blebs formed nearby, until the entire surface of the cell was covered with small blebs (Figure 4d, panels c,d). Within a relatively short time (less than an hour), the boundaries between individual blebs became obscured, producing what appeared to be large blebs extruding from a rounded cell body (Figure 4d, panels d,e). Finally, the cell appeared round with large, flat petal-like blebs (Figure 4d, panels e,f). Overall, this morphology differed from that observed in cells expressing the wild-type DAPk, in which the prominent phenotype was cell extensions and protrusions, followed later by retraction of these protrusions into large asymmetrical bulges. Additionally, the morphological changes induced by full-length DAPk occurred at a slower pace, over 5–6 h, whereas in DAPkΔCyto-expressing cells, the final blebbed state was achieved in 3 h or less. The deletion constructs exhibited similar distinct phenotypes in 293 cells as well (data not shown). Thus, the specific cellular localization of DAPk is critical for inducing the full repertoire of morphologic changes.

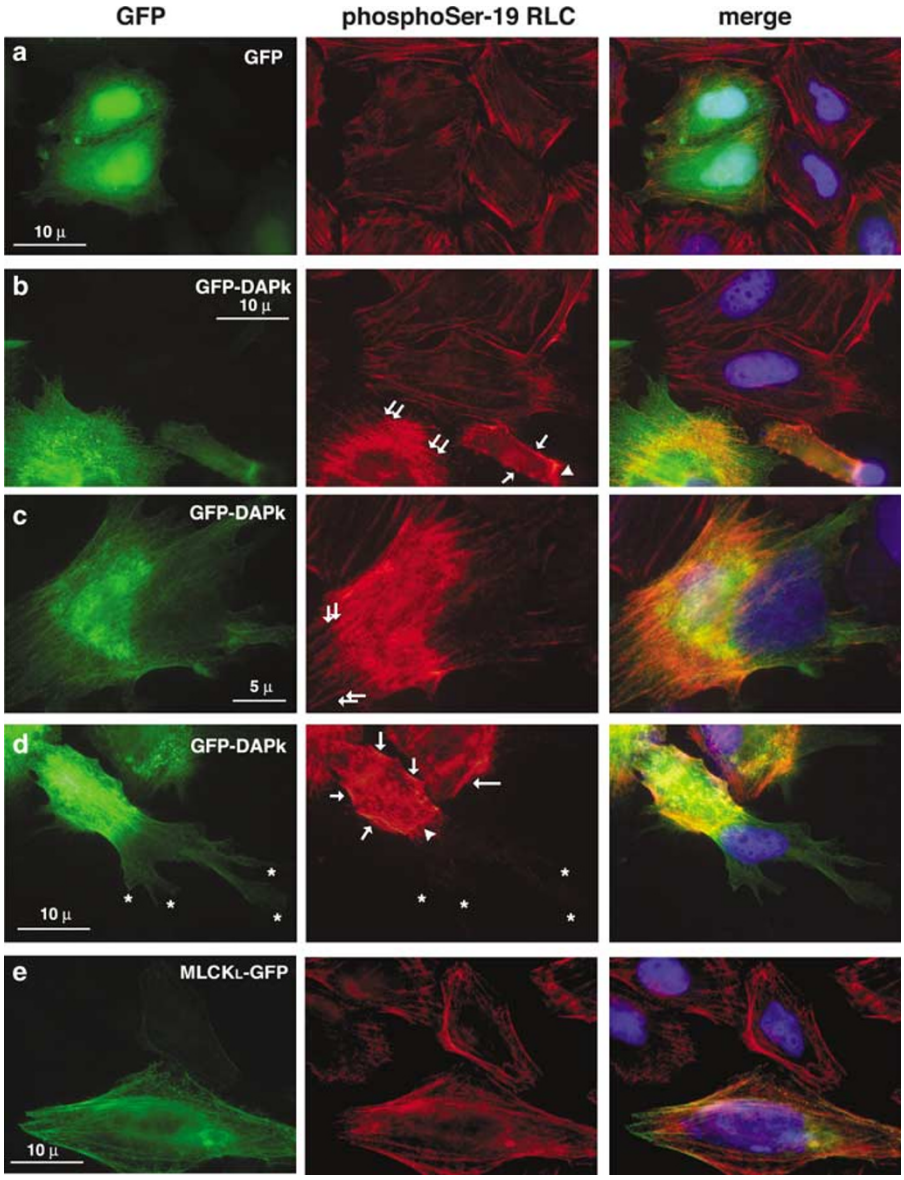

Figure 5 Induction and localization of phosphorylated RLC upon expression of DAPk. GFP alone (**a**), GFP–DAPk (**b–d**)-, or long MLCK–GFP (**e**)-transfected cells were fixed and costained with a phospho-Ser-19 RLC antibody and rhodamine-conjugated secondary antibody. Note the increase in phospho-RLC in DAPk-transfected cells *versus* nontransfected cells in the same field (**b**). Examples of staining at stress fibers (double arrows), cortical filaments (single arrows), and the necks of protrusions (arrowheads) are indicated. Protrusions are demarked with asterisks. Left: GFP channels, middle: rhodamine channel and right: merged image, including DAPI-stained nuclei

DAPk phosphorylates RLC *in vivo* and affects myosin distribution

The membrane blebbing that occurs during apoptosis involves activation of myosin-II by phosphorylation of the RLC.[26,27] The cellular contractions induced by DAPk expression may involve a similar mechanism. In fact, the most prominent *in vitro* substrate for DAPk is the RLC. Costaining for phospho-Ser-19 RLC was performed to determine if increased phosphorylated myosin-II correlates with DAPk expression and localization. Ser-19-phosphorylated RLC was observed in stress fibers in untransfected or GFP-transfected spread cells (Figure 5a,b), and at the leading edge of polarized cells (data not shown). Significantly, GFP–DAPk-expressing cells exhibited a marked enhancement in the intensity of the phospho-RLC staining (Figure 5b–d). In cells with little apparent morphological changes, increased phospho-RLC was observed in stress fibers in areas of high DAPk expression (Figure 5b,c, e.g. double arrows). Even upon treatment of cells with latrunculin B to depolymerize the actin filaments, the aggregates of GFP–DAPk (described in Figure 2) colocalized with the phosphorylated RLC (data not shown). Phosphorylated RLC was also particularly abundant in cells that displayed the DAPk-induced morphological changes; however, these cells had fewer stress fibers and instead displayed an accumulation of phospho-RLC at cortical

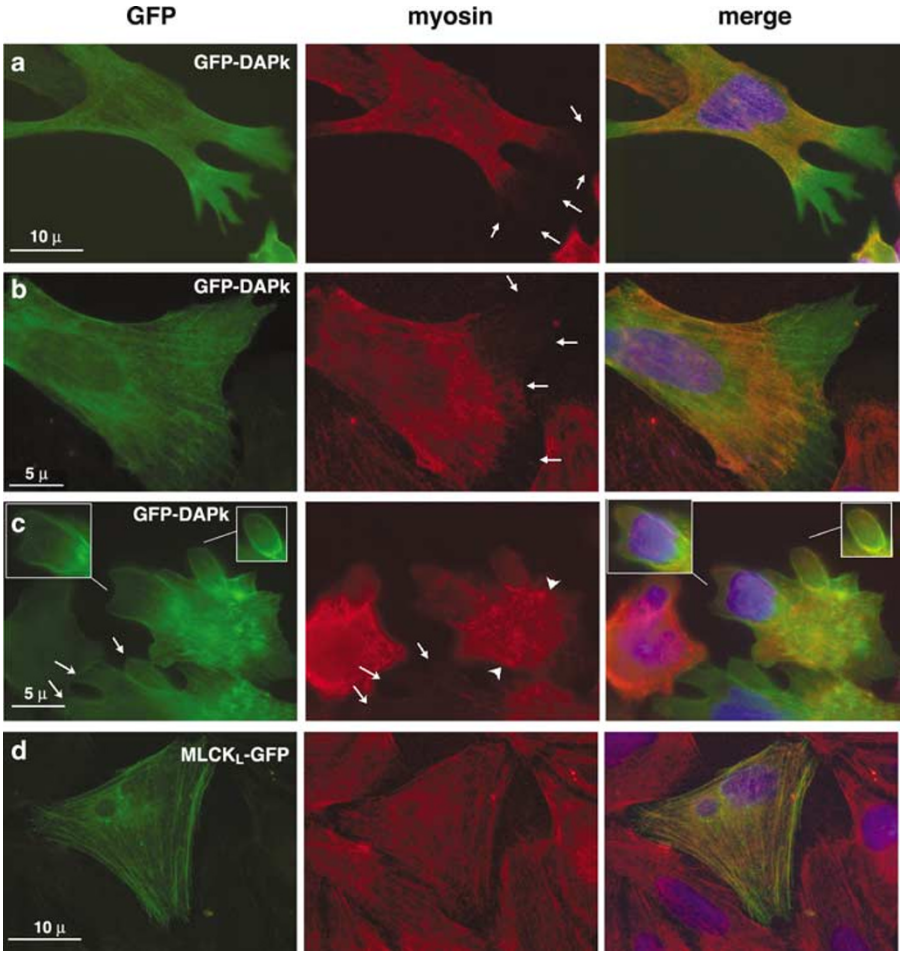

Figure 6 DAPk causes a redistribution of myosin-II. GFP–DAPk (**a–c**)-, or long MLCK–GFP (**d**)-transfected cells were fixed and costained with an antimyosin heavy chain antibody and rhodamine-conjugated secondary antibody. Cells exhibiting early stages (**a, b**) and late stages (**c**) of DAPk-induced morphologic changes are shown. Arrows in (**a–c**) demarcate the edges of the protrusions, from which myosin-II is excluded. Arrowheads in (**c**) indicate myosin staining in the central portion of cell. Left, GFP channel; middle, rhodamine channel; and right, merged image, including DAPI-stained nuclei

filaments and at the neck of protrusions (Figure 5b,d, single arrows and arrowhead, respectively). Interestingly, phosphorylated RLC was excluded from the protrusions (Figure 5d, asterisks).

A similar localization pattern was observed for myosin-II. Staining for myosin-II showed both a diffuse, unorganized localization as well as a stress fiber distribution (Figure 6a,b). The latter pattern showed a limited degree of overlap with GFP–DAPk localization, particularly in the mid portion of the cell body (Figure 6a,b). However, as in the case of phospho-RLC, the edges of the cell were devoid of myosin staining (e.g. Figure 6a,b, arrows). This contrasts with the localization of GFP–DAPk and actin filaments (not shown), which extend to the edges of the cell into the protrusions. Examination of cells in progressive stages of morphologic change confirmed this observation. At early stages, myosin-II was prominently excluded from cell protrusions, although these regions were rich in GFP–DAPk (Figure 6a, arrows). As the cells became more rounded, intense myosin-II staining was observed in the central region of the cell (Figure 6c, arrowheads), while the bulges displayed little myosin-II staining (Figure 6c, arrows). GFP–DAPk was observed along the periphery of individual bulges, and the basal portions of these bulges overlapped with myosin-II (e.g. panel c, inset). This staining pattern differed from that observed upon overexpression of long MLCK–GFP. MLCK also led to increased RLC phosphorylation on stress fibers, which overlapped almost completely with MLCK localization (Figure 5e). However, the phospho-RLC and myosin II (Figure 6d) were evenly distributed along the length of the stress fibers to the cell edge; in contrast with DAPk-expressing cells, no redistribution of myosin-II was observed. Thus, DAPk, but not MLCK, leads to significant reorganization of myosin-II and phosphorylation of the RLC, particularly in the mid portion of the cell body. This presumably induces myosin-II-mediated contractility from the center of the cell, which results in the extrusion of protrusions.

To confirm the observed increase in DAPk-induced RLC phosphorylation *in vivo*, Western blotting was performed. To increase the proportion of DAPk-expressing blebbing cells, DAPkΔCaM, a constitutively activated kinase, was introduced into the more transfectable 293T cells. Cellular extracts from DAPkΔCaM or luciferase transfectants were separated by urea-glycerol gel electrophoresis to resolve unphosphorylated and phosphorylated RLCs (Figure 7a). The majority of the

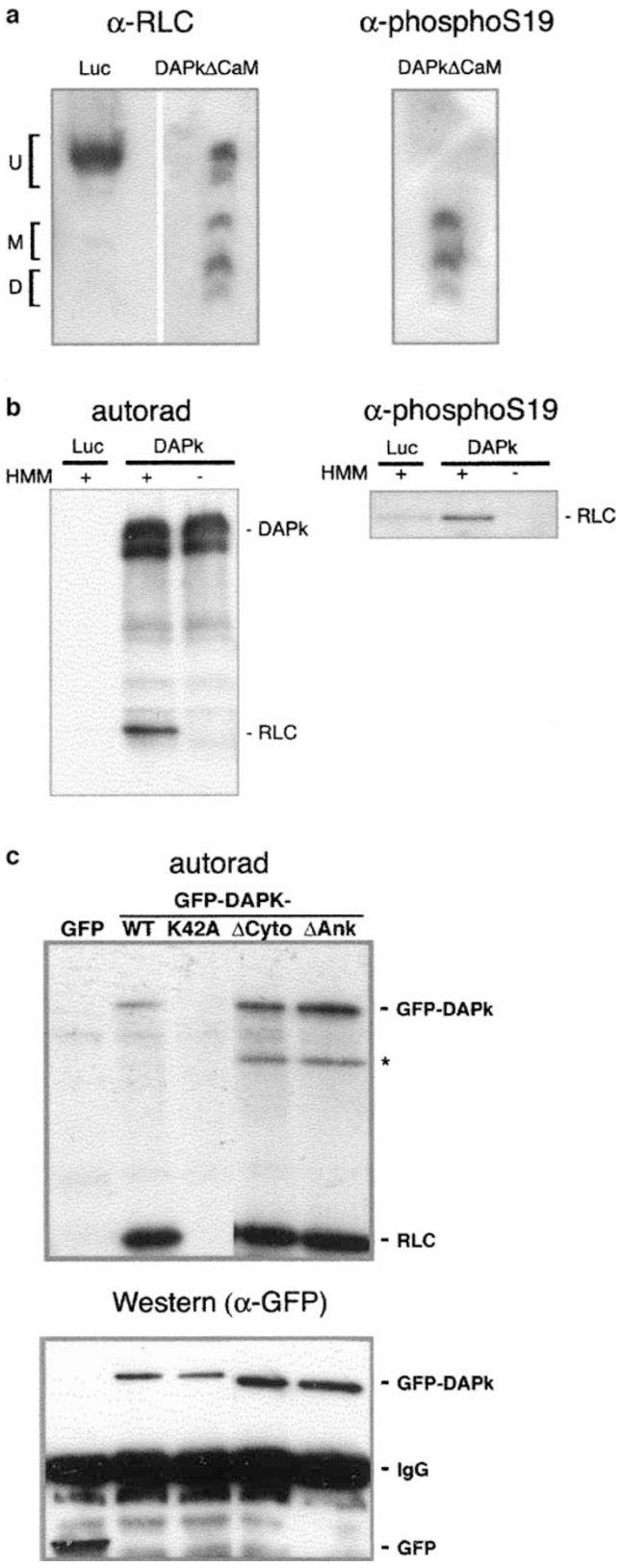

RLC in control cells was unphosphorylated. In contrast, in cells expressing active DAPk, the ratio of phopshorylated to unphosphorylated RLC increased, and both monophosphorylated and diphosphorylated RLCs were abundant, accounting for 45% of the total RLC. Moreover, an immunoblot with a phospho-Ser-19 antibody confirmed that Ser-19 was the site of phosphorylation.

These experiments indicate that DAPk leads to increased RLC phosphorylation *in vivo*, either directly or indirectly. In fact, DAPk is capable of directly phosphorylating the isolated RLC *in vitro.*[1] Since many protein kinases can phosphorylate the isolated RLC, but not heavy chain associated RLC, we examined the phosphorylation of heavy meromyosin by human DAPk. As shown in Figure 7b, the RLC within the complex is phosphorylated by Flag-HA-DAPk immunoprecipitated from cell lysates, but not by the control immunoprecipitate. An immunoblot with the phospho-Ser-19-specific antibody indicated that DAPk phosphorylates the RLC on Ser-19. Consistent with these results, previous studies have indicated that the murine form of DAPk phosphorylates recombinant RLC on Thr-18 and Ser-19, and intact myosin-II *in vitro*.[28]

Although DAPk is capable of directly phosphorylating the RLC *in vitro*, these results cannot exclude the possibility that *in vivo*, the phosphorylation is indirect, through DAPk-dependent activation of some other RLC kinase. The most likely candidate is the Rho-activated kinase, ROCK, which has been shown to mediate RLC phosphorylation and apoptotic membrane blebbing following cleavage by caspases.[27,29] ROCK induction of RLC phosphorylation can result not only from its ability to directly phosphorylate the light chain[30–32] but also from its ability to phosphorylate and inhibit the myosin binding subunit (MBS) of the myosin phosphatase.[33,34] We therefore examined the phosphorylation status of RLC in GFP–DAPk-transfected cells in the presence of the ROCK inhibitor Y27632 or the caspase inhibitor zVAD-fmk. The ROCK inhibitor completely abolished the stress fiber staining for phosphorylated RLC observed in nontransfected or GFP-transfected cells (Figure 8a,b). In addition, cells lost their rigidity and polarity, and were spread with random projections of lamellipodia, as previously reported.[31,32,35] Significantly, however, strong phospho-RLC immunostaining was observed in cells expressing GFP–DAPk even upon inhibition of ROCK activity. Moreover, in the absence of active

Figure 7 DAPk phosphorylates the RLC *in vitro* and *in vivo*. (**a**) Urea–glycerol gel fractionation of myosin light chains extracted from 293 cells transfected with luciferase or DAPkΔCaM. The blot was probed with an antibody to total RLC (left), stripped and reprobed with an antibody to phospho-Ser-19 RLC (right). U, unphosphorylated RLC; M, monophosphorylated RLC; D, diphosphorylated RLC. A shorter exposure of the blot is shown for luciferase transfectants, to normalize for unequal protein loading. (**b**) Autoradiogram showing both DAPk autophosphorylation and RLC phosphorylation (top), and phospho-Ser-19 RLC immunoblot (bottom) of an *in vitro* kinase reaction performed with immunopurified DAPk and heavy meromyosin (HMM). (**c**) Kinase activity of DAPk mutants. GFP–DAPk, GFP–DAPk K42A, GFP–DAPkΔAnk and GFP–DAPkΔCyto were immunoprecipitated from 293 cell lysates and used in an *in vitro* reaction to which purified recombinant RLC was added. Upper panel shows autoradiograms indicating both DAPk autophosphorylation and RLC phosphorylation. Lower panel shows the corresponding Western blots with anti-GFP antibodies, indicating DAPk expression levels. Asterisk indicates DAPk degradation product seen in some experiments

ROCK-mediated phosphorylation, it became particularly apparent that the phospho-RLC mediated by DAPk localized to stress fibers (Figure 8b). Thus DAPk-induced RLC phosphorylation occurs independently of ROCK. Moreover, the presence of the ROCK inhibitor did not significantly affect the formation of DAPk-induced protrusions (e.g. in one representative experiment, the percent of cells exhibiting protrusions was 35 and 24%, in the DMSO and Y27632 treated cells, respectively). However, the degree of bulge formation was reduced (2.5% in the presence of Y27632, *versus* 55% in the presence of DMSO), probably because the total myosin phosphorylation was lower than normally seen when both ROCK and DAPk are active. It is also noteworthy that the DAPk-induced phosphorylation was sufficient to overcome the effects of ROCK inhibition on cell morphology (Figure 8b). Together, these data suggest that DAPk functional effects are not dependent on ROCK activity.

We also assessed the general caspase inhibitor, zVAD-fmk, and found that it did not prevent any of the DAPk-induced morphologic changes. Also, the increases in RLC phosphorylation were similar in the presence or absence of the caspase inhibitor (data not shown). Thus, DAPk-mediated phosphorylation of the RLC and subsequent morphologic changes occur independently of caspases. This is consistent with previous reports of the caspase-independent nature of DAPk-induced cell death.[10]

We next examined whether the mislocalized GFP–DAPk constructs induced phosphorylation of the RLC. Both constructs maintained catalytic activity *in vitro*, as evidenced by their ability to undergo autophosphorylation and to phosphorylate purified RLC (Figure 7c). This latter activity can be attributed directly to DAPk, and not to any co-associated kinase, as the immunoprecipitate of a catalytically inactive mutant, GFP–DAPk K42A, failed to phosphorylate the RLC. *In vivo*, however, the constructs had distinct effects on RLC phosphorylation. GFP–DAPkΔCyto mildly induced Ser-19 phosphorylation of RLC, even in cells that did not yet exhibit any sign of rounding or blebbing (Figure 9b). In blebbing cells, however, phospho-RLC was observed in a dot-like pattern and a ring at the cell periphery (Figure 9c, arrowheads). No phospho-RLC was observed within the blebs themselves (Figure 9c, arrows). The increase in RLC phosphorylation was observed even upon treatment with the ROCK inhibitor Y27632 (Figure 9d). However, in the absence of the basal ROCK-mediated phosphorylation, it was apparent that DAPkΔ Cyto-induced RLC phosphorylation localized in a diffuse pattern that was not associated with stress fibers. Consistent with its inability to restore RLC phosphorylation at stress fibers, GFP–DAPkΔCyto did not reverse the effect of ROCK inhibition on cell shape, and the cells failed to exhibit cell rounding and blebbing (Figure 9d). Significantly, in GFP–DAPkΔAnk-expressing cells, phospho-Ser-19-RLC was observed at levels that were comparable to those seen in nontransfected cells (Figure 9a). This is consistent with the lack of morphologic changes. Thus, the ability of the DAPk deletants to elicit morphological changes correlated with the level and location of RLC phosphorylation *in vivo*. This suggests that RLC phosphorylation, and the subsequent activation of myosin-II, is an important component of DAPk-mediated morphologic changes.

Discussion

DAPk-mediated cell death is characterized by two main characteristics: formation of autophagic vesicles and membrane blebbing.[10] Although these processes occur concurrently, they may represent independent functional arms of DAPk. Overexpression of DAPk leads to a reduction in cell number and overall colony growth,[1] presumably a result of the induction of autophagy. The contribution of blebbing to the terminal state is unknown. Yet, membrane blebbing is a phenomenon common to a vast majority of apoptotic stimuli. In this paper, we specifically examined the membrane blebbing arm of DAPk function, in a cell system where the death process is slow, so that morphologic changes can be

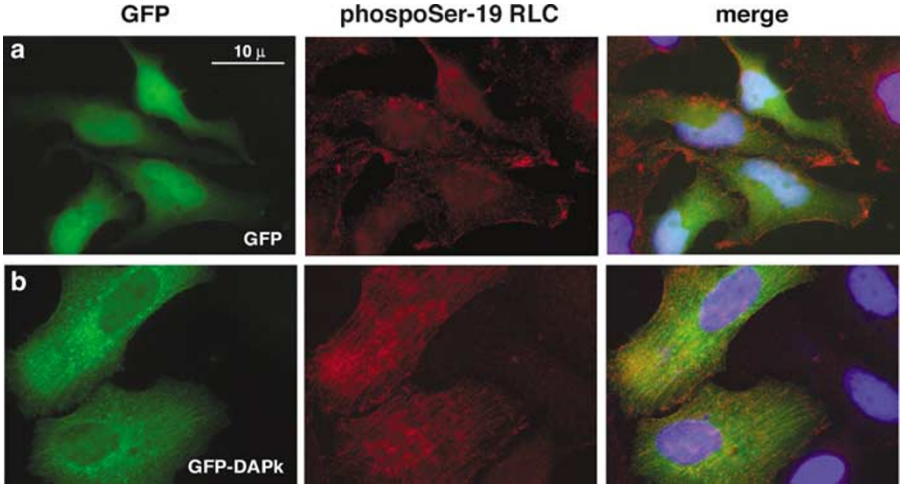

Figure 8 DAPk induces phosphorylation of RLC independently of ROCK. Cells transfected with GFP (**a**) or GFP–DAPk (**b**), in the presence of ROCK inhibitor Y27632 (10 μM), were fixed and costained with antiphospho-Ser-19 RLC antibody and rhodamine-conjugated secondary antibody. Left, GFP channels; middle, rhodamine channel; and right, merged image, including DAPI-stained nuclei. Scale bar shown in panel (**a**) applies to all panels

observed prior to the final death throes of the cell. To this end, we have fused GFP to DAPk to simultaneously visualize DAPk localization and examine its morphologic effects on the cell. We show that DAPk partially localizes to the actin cytoskeleton, in particular to stress fibers, and its expression correlates with increased *in vivo* phosphorylation of Ser-19 on the RLC of myosin-II. Furthermore, two protein domains, the previously characterized cytoskeletal interacting region (residues 641–835), and the eight ankyrin repeats (residues 365–629), are critical for proper localization of DAPk and its functional effects on cell morphology (see Table 1 for summary). The cytoskeletal interacting region provides the essential interaction with the actin cytoskeleton, so that in its absence, DAPk is completely cytoplasmic. However, this domain is not sufficient to direct the kinase along actin filaments; unless the ankyrin repeats are also present, DAPk loses, for the most part, its stress fiber localization, and instead accumulates at focal contacts. Thus, the ankyrin repeats are necessary for the interaction with actin stress fibers. The importance of this domain for the proper subcellular localization of the kinase might explain why expression of a fragment of the ankyrin repeat has inhibitory effects on DAPk's death-inducing abilities.[36]

In contrast to the results presented here, a recent study did not detect phosphorylation of the endogenous RLC (or death-associated phenotypic changes) upon overexpression of either of the two mouse DAPk isoforms.[28] A significant increase in RLC phosphorylation was observed, however, upon expression of the mouse DAPks in the presence of TNF-α. This discrepancy may be due to differences in cell types or expression levels achieved; in the previous report, a TNF-mediated activation step was likely required to activate the otherwise dormant kinases, while in our HeLa cells, overexpression of DAPk sufficed. On a cautionary note, overexpression may confer functional capabilities to DAPk that are not characteristic of the endogenous kinase. For lack of efficient antibodies to cellular DAPk, we could not compare the localization of the endogenous kinase to that of the GFP-fused kinase. However, we have previously shown that a dominant negative fragment of DAPk blocks blebbing in TNF-

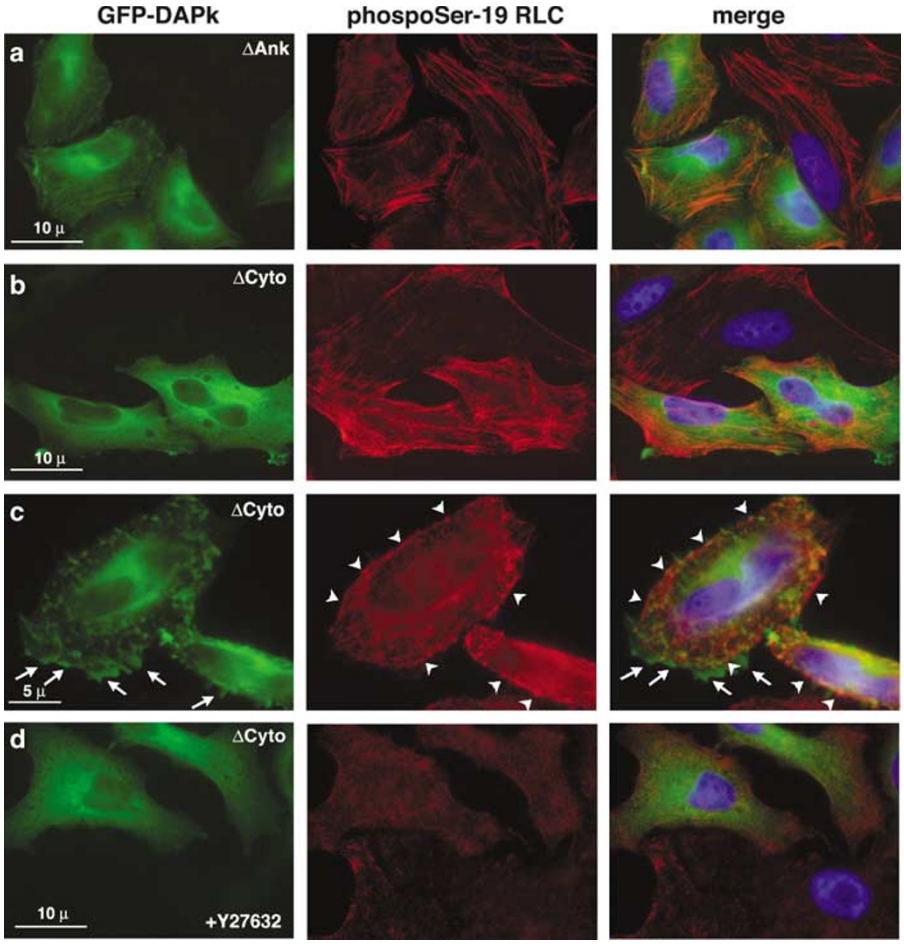

Figure 9 Induction and localization of phosphorylated RLC upon expression of DAPk mutants. DAPkΔAnk (**a**)- or GFP–DAPkΔCyto (**b–d**)-transfected cells were fixed and costained with a phospho-Ser-19 RLC antibody and rhodamine-conjugated secondary antibody. In (**d**), cells were treated with ROCK inhibitor Y27632 (10 μM). Arrows and arrowheads in (**c**) indicate blebs and peripheral phospho-RLC accumulation, respectively. Left, GFP channels; middle, rhodamine channel; and right, merged image, including DAPI-stained nuclei. Note: the appearance of bilobal nuclei that give the impression of multinucleation, such as seen in panels (**b**,**c**), is a common feature of these cells and cannot be attributed to expression of GFP–DAPkΔCyto

Table 1 Summary of GFP–DAPk and deletant mutants

	GFP–DAPk WT	GFP–DAPk ΔAnk	GFP–DAPk ΔCyto	$MLCK_L$–GFP
Ankyrin domain	+	−	+	NA
Cytoskeletal interacting domain	+	+	−	NA
In vitro kinase activity	+	+	+	+
Primary localization	Stress fibers, cortical actin filaments	Focal contacts	Diffuse in cytoplasm	Stress fibers
In vivo RLC phosphorylation	+	−	+	+
Morphology	Protrusions, large asymmetrical bulges	No effect	Cell rounding, small, spherical blebs	Thick stress fibers, rigid cell

NA = not applicable.

α-treated 293 cells,[10] providing strong support that the endogenous DAPk functions in myosin-mediated apoptotic membrane blebbing, and that the results reported here represent physiological processes.

DAPk phosphorylates the RLC of intact myosin-II *in vitro*, and induces phosho-RLC *in vivo*, supporting the hypothesis that DAPk directly mediates RLC phosphorylation *in vivo*. However, to date, a number of other RLC kinases have been proposed to mediate blebbing and RLC phosphorylation during apoptosis, in particular, MLCK and ROCK I.[26,27,29] It is formally possible that DAPk's effects on RLC are mediated through one or more of these kinases. However, the different phenotypes that result from expression of MLCK and DAPk suggest that DAPk does not function through activation of MLCK. Long MLCK–GFP induced the formation of thick actin stress fibers, and a slightly more rigid cell shape, but did not produce the protrusions and contractions that are characteristic of DAPk. We could not test whether DAPk-induced RLC phosphorylation continues to take place in the presence of MLCK inhibitors, since low molecular weight inhibitors of MLCK can inhibit DAPk as well (unpublished data). We have also excluded ROCK as the direct mediator, as we have shown by using the ROCK inhibitor that DAPk-mediated phosphorylation of RLC and cellular protrusions occur independently of ROCK. Yet, within the DAPk family itself, DRP-1 and ZIP-kinase are also capable of phosphorylating the purified regulatory light chain.[2,3,5,6] In fact, ZIPk phosphorylates the RLC on Thr18 and Ser19 *in vivo*, leading to membrane protrusions that are reminiscent of those observed with DAPk.[37] In addition, introduction of RLC mutated at Thr18 and Ser19 blocked ZIPk-induced protrusions.[37] The similarity between the effects of the two kinases suggests that ZIPk and DAPk have similar functions. Alternatively, they may act in a cascade, whereby one kinase activates the second (Shani G and Kimchi A unpublished data). Thus, we presently cannot exclude the possibility that, *in vivo*, DAPk leads to RLC phosphorylation through activation of ZIPk. Nevertheless, these results indicate that DAPk, perhaps with the assistance of its family members, is capable of phosphorylating the RLC and mediating membrane protrusions independently of ROCK and MLCK.

RLC phosphorylation and the resultant contractile forces generated by the acto-myosin network at the cortical actin ring are believed to play a central role in mediating apoptotic membrane blebbing.[38] In fact, DAPk-expressing cells display global contractions that produce extrusions from the cell body and large, asymmetrical bulges, which most likely result from the activation of myosin-II, in particular following its reorganization to the central portion of the cell. The severity of the phenotype, which reflects the contractile state of the cell, correlates with the extent and location of RLC phosphorylation. The greatest contractility is observed with the wild-type DAPk, which induces increased phosho-RLC at stress fibers. This reflects the fact that DAPk resides at stress fibers, in close proximity to myosin-II, and perhaps, additional actin-associated substrates. An intermediate state is achieved with the exclusively cytoplasmic DAPkΔCyto; it also phosphorylates the RLC *in vivo*, but not at stress fibers. Thus, ectopic localization to the cytosol may interfere with DAPk's ability to phosphorylate stress-fiber associated substrates. Furthermore, cytoplasmic localization of DAPk may expose it to novel substrates that the stress-fiber associated kinase does not encounter. This altered substrate profile might explain why GFP–DAPkΔCyto triggers symmetrical, peripheral membrane blebbing, in the absence of cell contractions and protrusions. Lastly, DAPkΔAnk, which accumulates at focal contacts, has no effect on the basal contractile state of the cell and no abnormal morphologies are seen upon its expression. This may be related to its inability to induce RLC phosphorylation *in vivo*. The lack of phosphorylation suggests that GFP–DAPkΔAnk, *in vivo*, is a relatively inefficient RLC kinase, although it maintains *in vitro* kinase activity. The simplest explanation for this impaired functional activity is that its sequestration to the focal contacts precludes it from phosphorylating the relevant DAPk substrates. We cannot, however, exclude the possibility that deletion of the ankyrin repeats affects its folding or its interactions with some other factors that influence its function. Resolution of this matter awaits the identification of additional substrates and interacting partners of DAPk.

Inhibition of ROCK leads to total suppression of RLC phosphorylation and a hypocontractile state in which the cells are randomly spread. Expression of WT DAPk in the presence of the ROCK inhibitor restores both RLC phosphorylation and the basal contractile state, with a limited degree of hypercontractility. In contrast, expression of the ΔCyto construct does not restore contractility to the cell, although it is capable of inducing phosphorylation of the RLC. This may be due to the

fact that in this case, the phospho-RLC is localized in a diffuse manner, and not at stress fibers. It is interesting that WT DAPk can rescue the effects of ROCK inhibition, even though ROCK's cytoskeletal functions are mediated by multiple substrates, in addition to the myosin-II RLC and its phosphatase.[39] Either lack of RLC phosphorylation is the most significant factor that contributes to the hypocontractile phenotype, or WT DAPk and ROCK share additional substrates.

Thus, DAPk joins the list of RLC kinases that are involved in regulating morphologic changes associated with cell death. The precise roles of the multiple RLC kinases in mediating apoptotic membrane blebbing still remain to be determined. Although it is possible that they have redundant, overlapping functions, the multiple kinases could serve as sensors for particular signals, leading to similar outcomes in different cell environments. Specifically, the kinases can be activated by different mechanisms, including changes in cellular Ca^{2+} (MLCK, DAPk, DRP-1), dephosphorylation (DAPk, DRP-1),[40,41] or caspase-mediated cleavage (ROCK1).[27,29] Furthermore, functional domains outside the catalytic domains differ greatly among the various kinases, and unique regions, such as DAPk's death domain, or MLCK's N-terminal Ig motifs, may contribute to the regulation or activity of each kinase. Thus, the presence of multiple RLC kinases, poised to respond to different signals, may produce a more efficient mechanism for generating membrane blebs.

Materials and Methods

Plasmid construction

Plasmids encoding N-terminal FLAG and HA-tagged human full-length DAPk (pcDNA3-DAPk), or the activated kinase deleted of its CaM regulatory domain (pcDNA3-DAPkΔCaM), luciferase (pcDNA3-Luc) and nonmuscle long MLCK fused with GFP at its C-terminus (pMLCK$_L$-GFP) have been described previously.[1,24] In-frame C-terminal fusions of GFP to full-length DAPk, or the catalytically inactive K42A mutant, were generated by excising the 4.7 kB *Eco*R1 fragment encoding HA-tagged DAPk from pcDNA3-DAPk or pcDNA3-DAPk K42A[1] and inserting it into pEGFP-C2 (Clontech), to produce pEGFP-DAPk or pEGFP-DAPk K42A, respectively. A construct in which the DAPk cassette was inserted in the reverse orientation was used as a control for a GFP-expressing plasmid of identical size that does not produce a fusion protein (pEGFP-DAPk(rev)). pEGFP-DAPkΔCyto was generated by subcloning the 4.1 kB *Eco*RI fragment encoding HA-tagged DAPk lacking the cytoskeletal interacting region (amino acids 641–835) from pcDNA3-DAPkΔCyto[1] to pEGFP-C2. To generate pEGFP-DAPkΔAnk, a 1.6 kB *Eco*RV/*Xba*I fragment encompassing the ankyrin repeats was excised from pEGFP-DAPk and inserted into pBluescript II KS (Stratagene). An in-frame deletion of the ankyrin repeats and the neighboring P loop (amino acids 365–641) was obtained by digestion with *Bgl*II and *Hpa*I, followed by religation. The new 750 bp *Eco*RV/*Xba*I fragment containing the deletion was then reinserted into the original pEGFP-DAPk.

Cell lines, transfections and live imaging

293T human embryonic kidney cells and HeLa cells[24] were grown in DMEM (Biological Industries) supplemented with 10% fetal bovine serum (Sigma), L-glutamine (2 mM), penicillin (50 U/ml), and streptomycin (50 μg/ml, Gibco BRL). Cells were transiently transfected by the Ca^{2+}-phosphate precipitation method. Where indicated, cells were treated with 100 μM zVAD-fmk (Enzyme Systems Products) or 10 μM Y27632 (Calbiochem) at the time of transfection. For live imaging of HeLa cells, 0.8–1.0 $\times$ 10^5 cells were grown on 3.5 cm tissue culture plates containing embedded gridded coverslips (Bellco), transfected with 3.5 μg GFP–DAPk or unfused GFP-expressing plasmids and viewed 15–24 h later on an inverted IX70 fluorescent microscope (Olympus) equipped with a PlanApo 60 $\times$ oil immersion objective (NA 1.4) and a digital camera (DVC). For each field viewed, the region of the grid was noted and the same field was re-examined and imaged multiple times for up to 6 h. For actin depolymerization experiments, cells that had been viewed and photographed were incubated for 30 min with either 5 μM latrunculin B (Sigma) or as a control, DMSO (0.05%), and reimaged. The treatment media was then removed, cells were washed with growth media, allowed to recover for 30 min under normal growth conditions, and imaged a final time.

Immunostaining

For focal contact and phospho-Ser-19 RLC immunostaining, transfected cells grown on coverslips were fixed in 3.7% formaldehyde for 15 min and permeabilized/blocked with 0.4% Triton-X 100 (Sigma), 10% normal goat serum (Biological Industries). Cells were then incubated with a monoclonal anti-paxillin antibody (1 : 200, BD Transduction Laboratories) or a rabbit polyclonal anti-phospho-RLC2 (Ser-19) antibody (1 : 200, Cell Signaling Technology) followed by rhodamine-conjugated anti-mouse or anti-rabbit secondary antibodies, respectively (1 : 800 or 1 : 400, Jackson ImmunoResearch). For myosin staining, cells were fixed in methanol for 15 min at -20°C, permeabilized and blocked as above, and incubated with a rabbit polyclonal anti-myosin heavy chain antibody (1 : 150, BTI), followed by rhodamine-conjugated anti-rabbit secondary antibody (1 : 800). In all cases, cells were incubated in parallel with secondary antibody alone, so that the specificity of the staining could be verified. For visualization of actin, cells were gently permeabilized in Buffer M (0.1% Triton X-100, 50 mM imidazole pH 6.8, 50 mM KCl, 0.5 mM $MgCl_2$, 1 mM β-mercaptoethanol, 1 mM EGTA, 2% PEG 20 000, plus protease inhibitors)[42] and then fixed in formaldehyde and stained with Texas Red-X-conjugated phalloidin (1 : 200, Molecular Probes) for 1 h. All coverslips were finally stained with DAPI (0.5 μg/ml, Sigma) and mounted in Fluoromount G (Southern Biotechnology Associates) embedding media. Stained cells were viewed by fluorescent microscopy with 60 $\times$ or 100 $\times$ oil immersion objectives (Olympus BX41). Digital imaging was performed with a DP50 CCD camera using Viewfinder Lite and Studio Lite software (Olympus). Where indicated, cells were viewed by confocal laser scanning microscopy (BioRad Radiance 2100, mounted on Nikon TE300). Final composites for all images were prepared in Adobe Photoshop (Adobe Systems).

Kinase assays

293T cells expressing GFP–DAPk constructs were lysed in PLB buffer, supplemented with protease and phosphatase inhibitors as described previously.[43] Extracts were immunoprecipitated by incubation for 2 h at 4°C with an anti-HA monoclonal antibody (Babco, HA.11) conjugated to protein G beads (Santa Cruz). Beads were washed repeatedly with PLB buffer, followed by two washes in kinase buffer (50 mM Hepes pH 7.5, 20 mM $MgCl_2$, 0.1 mg/ml BSA). Immunoprecipitates were incubated for 5 min at 30°C in 30 μl kinase buffer containing 5–9 μCi [γ-^{32}P]ATP (1–1.8 pmol), 50 μM ATP, 1 μM bovine CaM (Sigma), 0.5 mM $CaCl_2$, and

1.6 μM recombinant human RLC (kind gift of M Gautel, EMBL, Heidelberg Germany). For analysis of phosphorylation of intact myosin, FLAG/HA-tagged DAPk and luciferase expressed in 293T cells were immunoprecipitated using anti-Flag monoclonal antibodies coupled to agarose beads (M_2 affinity gel; IBI Kodak). The kinase reaction was performed for 30 min as above with 0.14 μM of recombinant chicken nonmuscle heavy meromyosin-IIB (kind gift of R Adelstein, NIH, Bethesda, MD, USA[44]). Reactions were terminated by boiling in SDS-loading buffer, resolved on 10% acrylamide gels and transferred to nitrocellulose membranes. Membranes were exposed to film to obtain autoradiograms, and then subjected to Western blotting as described below.

Western blot analysis

Kinase assays or total cell extracts were separated by standard SDS-PAGE on 10% gels. Blots were reacted with either monoclonal antibody to GFP (Babco, 1 : 5000), polyclonal anti-RLC antibody[28] (kind gift of P Gallagher, Indiana University School of Medicine, Indianapolis, IN, USA, 1 : 3000) or polyclonal pp2b antibody, which specifically recognizes phosphorylated Ser-19 on RLC[45] (1 : 200, kind gift of F Matsumura, Rutgers U, Piscataway, NJ, USA), followed by HRP-conjugated goat anti-mouse (1 : 10 000) or anti-rabbit (1 : 40 000) secondary antibody (Jackson ImmunoResearch), as appropriate, and detected by standard enzyme-linked chemiluminescence (Pierce).

In vivo RLC phosphorylation analysis

293 cells were transfected with pcDNA3-Luc or pcDNA3-DAPkΔCaM and approximately 24 h later, protein was extracted in cold 10% TCA, 10 mM DTT. Pellets were washed in acetone and resuspended in 8 M urea buffer, 20 mM Tris pH 8.6, 22 mM glycine, 10 mM DTT, 0.004% bromophenol blue. Myosin light chains were resolved by urea–glycerol gel electrophoresis as described,[46] and transferred to nitrocellulose membranes, which were reacted for total and phosphorylated RLC as described above.

Acknowledgements

We gratefully acknowledge Y Zwang for assistance with molecular cloning, B Geiger and A Bershadsky for access to reagents and insightful discussions, and members of the Kimchi lab for critical reading of the manuscript and helpful suggestions. We also thank M Gautel (EMBL, Heidelberg Germany), R Adelstein (NIH, Bethesda, MD, USA), P Gallagher (Indiana University School of Medicine, Indianapolis, IN, USA), and F Matsumura (Rutgers U., Piscataway, NJ, USA) for their generosity in providing reagents listed in the Material and Methods. This work was supported by a grant from DIP (Deutsch-Israelische Projektkooperation) and by the Feinberg Foundation. AK is the incumbent of the Helena Rubinstein Chair of Cancer Research. ARB is supported by a grant from the National Institutes of Health.

References

1. Cohen O, Feinstein E and Kimchi A (1997) DAP-kinase is a Ca^{2+}/calmodulin-dependent, cytoskeletal-associated protein kinase, with cell death-inducing functions that depend on its catalytic activity. EMBO J. 16: 998–1008
2. Inbal B, Shani G, Cohen O, Kissil JL and Kimchi A (2000) Death-associated protein kinase-related protein 1, a novel serine/threonine kinase involved in apoptosis. Mol. Cell. Biol. 20: 1044–1054
3. Kawai T, Nomura F, Hoshino K, Copeland NG, Gilbert DJ, Jenkins NA and Akira S (1999) Death-associated protein kinase 2 is a new calcium/calmodulin-dependent protein kinase that signals apoptosis through its catalytic activity. Oncogene 18: 3471–3480
4. Kawai T, Matsumoto M, Takeda K, Sanjo H and Akira S (1998) ZIP kinase, a novel serine/threonine kinase which mediates apoptosis. Mol. Cell. Biol. 18: 1642–1651
5. Kogel D, Plottner O, Landsberg G, Christian S and Scheidtmann KH (1998) Cloning and characterization of Dlk, a novel serine/threonine kinase that is tightly associated with chromatin and phosphorylates core histones. Oncogene 17: 2645–2654
6. Murata-Hori M, Suizu F, Iwasaki T, Kikuchi A, Hosoya H, Burgering BM and Evan GI (1999) ZIP kinase identified as a novel myosin regulatory light chain kinase in HeLa cells. FEBS Lett. 451: 81–84
7. Cohen O, Inbal B, Kissil JL, Raveh T, Berissi H, Spivak-Kroizaman T, Feinstein E and Kimchi A (1999) DAP-kinase participates in TNF-alpha- and Fas-induced apoptosis and its function requires the death domain. J. Cell Biol. 146: 141–148
8. Inbal B, Cohen O, Polak-Charcon S, Kopolovic J, Vadai E, Eisenbach L and Kimchi A (1997) DAP kinase links the control of apoptosis to metastasis. Nature 390: 180–184
9. Raveh T, Droguett G, Horwitz MS, DePinho RA and Kimchi A (2001) DAP kinase activates a p19ARF/p53-mediated apoptotic checkpoint to suppress oncogenic transformation. Nat. Cell Biol. 3: 1–7
10. Inbal B, Bialik S, Sabanay I, Shani G and Kimchi A (2002) DAP kinase and DRP-1 mediate membrane blebbing and the formation of autophagic vesicles during programmed cell death. J. Cell Biol. 157: 455–468
11. Yamamoto M, Hioki T, Ishii T, Nakajima-Iijima S and Uchino S (2002) DAP kinase activity is critical for C(2)-ceramide-induced apoptosis in PC12 cells. Eur. J. Biochem. 269: 139–147
12. Pelled D, Raveh T, Riebeling C, Fridkin M, Berissi H, Futerman AH and Kimchi A (2002) Death-associated protein (DAP) kinase plays a central role in ceramide-induced apoptosis in cultured hippocampal neurons. J. Biol. Chem. 277: 1957–1961
13. Jang CW, Chen CH, Chen CC, Chen JY, Su YH and Chen RH (2002) TGF-beta induces apoptosis through Smad-mediated expression of DAP-kinase. Nat. Cell Biol. 4: 51–58
14. Kissil JL, Feinstein E, Cohen O, Jones PA, Tsai YC, Knowles MA, Eydmann ME and Kimchi A (1997) DAP-kinase loss of expression in various carcinoma and B-cell lymphoma cell lines: possible implications for role as tumor suppressor gene. Oncogene 15: 403–407
15. Raveh T and Kimchi A (2001) DAP kinase-a proapoptotic gene that functions as a tumor suppressor. Exp. Cell Res. 264: 185–192
16. Satoh A, Toyota M, Itoh F, Kikuchi T, Obata T, Sasaki Y, Suzuki H, Yawata A, Kusano M, Fujita M, Hosokawa M, Yanagihara K, Tokino T and Imai K (2002) DNA methylation and histone deacetylation associated with silencing DAP kinase gene expression in colorectal and gastric cancers. Br. J. Cancer 86: 1817–1823
17. Simpson DJ, Clayton RN and Farrell WE (2002) Preferential loss of death associated protein kinase expression in invasive pituitary tumours is associated with either CpG island methylation or homozygous deletion. Oncogene 21: 1217–1224
18. Tada Y, Wada M, Taguchi K, Mochida Y, Kinugawa N, Tsuneyoshi M, Naito S and Kuwano M (2002) The association of death-associated protein kinase hypermethylation with early recurrence in superficial bladder cancers. Cancer Res. 62: 4048–4053
19. Wong TS, Chang HW, Tang KC, Wei WI, Kwong DL, Sham JS, Yuen AP and Kwong YL (2002) High frequency of promoter hypermethylation of the death-associated protein-kinase gene in nasopharyngeal carcinoma and its detection in the peripheral blood of patients. Clin. Cancer Res. 8: 433–437
20. Kim DH, Nelson HH, Wiencke JK, Christiani DC, Wain JC, Mark EJ and Kelsey KT (2001) Promoter methylation of DAP-kinase: association with advanced stage in non-small cell lung cancer. Oncogene 20: 1765–1770
21. Maruyama R, Toyooka S, Toyooka KO, Virmani AK, Zochbauer-Muller S, Farinas AJ, Minna JD, McConnell J, Frenkel EP and Gazdar AF (2002) Aberrant promoter methylation profile of prostate cancers and its relationship to clinicopathological features. Clin. Cancer Res. 8: 514–519
22. Tang X, Khuri FR, Lee JJ, Kemp BL, Liu D, Hong WK and Mao L (2000) Hypermethylation of the death-associated protein (DAP) kinase promoter and aggressiveness in stage I non-small-cell lung cancer. J. Natl. Cancer Inst. 92: 1511–1516

23. Bresnick AR (1999) Molecular mechanisms of nonmuscle myosin-II regulation. Curr. Opin. Cell Biol. 11: 26–33
24. Poperechnaya A, Varlamova O, Lin PJ, Stull JT and Bresnick AR (2000) Localization and activity of myosin light chain kinase isoforms during the cell cycle. J. Cell Biol. 151: 697–708
25. Blue EK, Goeckeler ZM, Jin Y, Hou L, Dixon SA, Herring BP, Wysolmerski RB and Gallagher PJ (2002) 220- and 130-kDa MLCKs have distinct tissue distributions and intracellular localization patterns. Am. J. Physiol. Cell Physiol. 282: C451–C460
26. Mills JC, Stone NL, Erhardt J and Pittman RN (1998) Apoptotic membrane blebbing is regulated by myosin light chain phosphorylation. J. Cell Biol. 140: 627–636
27. Sebbagh M, Renvoize C, Hamelin J, Riche N, Bertoglio J and Breard J (2001) Caspase-3-mediated cleavage of ROCK I induces MLC phosphorylation and apoptotic membrane blebbing. Nat. Cell Biol. 3: 346–352
28. Jin Y, Blue EK, Dixon S, Hou L, Wysolmerski RB and Gallagher PJ (2001) Identification of a new form of death-associated protein kinase that promotes cell survival. J. Biol. Chem. 276: 39667–39678
29. Coleman ML, Sahai EA, Yeo M, Bosch M, Dewar A and Olson MF (2001) Membrane blebbing during apoptosis results from caspase-mediated activation of ROCK I. Nat. Cell Biol. 3: 339–345
30. Amano M, Ito M, Kimura K, Fukata Y, Chihara K, Nakano T, Matsuura Y and Kaibuchi K (1996) Phosphorylation and activation of myosin by Rho-associated kinase (Rho-kinase). J. Biol. Chem. 271: 20246–20249
31. Totsukawa G, Yamakita Y, Yamashiro S, Hartshorne DJ, Sasaki Y and Matsumura F (2000) Distinct roles of ROCK (Rho-kinase) and MLCK in spatial regulation of MLC phosphorylation for assembly of stress fibers and focal adhesions in 3T3 fibroblasts. J. Cell Biol. 150: 797–806
32. Ueda K, Murata-Hori M, Tatsuka M and Hosoya H (2002) Rho-kinase contributes to diphosphorylation of myosin II regulatory light chain in nonmuscle cells. Oncogene 21: 5852–5860
33. Kawano Y, Fukata Y, Oshiro N, Amano M, Nakamura T, Ito M, Matsumura F, Inagaki M and Kaibuchi K (1999) Phosphorylation of myosin-binding subunit (MBS) of myosin phosphatase by Rho-kinase in vivo. J. Cell Biol. 147: 1023–1038
34. Kimura K, Ito M, Amano M, Chihara K, Fukata Y, Nakafuku M, Yamamori B, Feng J, Nakano T, Okawa K, Iwamatsu A and Kaibuchi K (1996) Regulation of myosin phosphatase by Rho and Rho-associated kinase (Rho-kinase). Science 273: 245–248
35. Worthylake RA and Burridge K (2003) RhoA and ROCK promote migration by limiting membrane protrusions. J. Biol. Chem. 278: 13578–13584
36. Raveh T, Berissi H, Eisenstein M, Spivak T and Kimchi A (2000) A functional genetic screen identifies regions at the C-terminal tail and death-domain of death-associated protein kinase that are critical for its proapoptotic activity. Proc. Natl. Acad. Sci. USA 97: 1572–1577
37. Murata-Hori M, Fukuta Y, Ueda K, Iwasaki T and Hosoya H (2001) HeLa ZIP kinase induces diphosphorylation of myosin II regulatory light chain and reorganization of actin filaments in nonmuscle cells. Oncogene 20: 8175–8183
38. Mills JC, Stone NL and Pittman RN (1999) Extranuclear apoptosis. The role of the cytoplasm in the execution phase. J. Cell Biol. 146: 703–708
39. Amano M, Fukata Y and Kaibuchi K (2000) Regulation and functions of Rho-associated kinase. Exp. Cell Res. 261: 44–51
40. Shani G, Henis-Korenblit S, Jona G, Gileadi O, Eisenstein M, Ziv T, Admon A and Kimchi A (2001) Autophosphorylation restrains the apoptotic activity of DRP-1 kinase by controlling dimerization and calmodulin binding. EMBO J. 20: 1099–1113
41. Shohat G, Spivak-Kroizman T, Cohen O, Bialik S, Shani G, Berrisi H, Eisenstein M and Kimchi A (2001) The pro-apoptotic function of death-associated protein kinase is controlled by a unique inhibitory autophosphorylation-based mechanism. J. Biol. Chem. 276: 47460–47467
42. Tint IS, Hollenbeck PJ, Verkhovsky AB, Surgucheva IG and Bershadsky AD (1991) Evidence that intermediate filament reorganization is induced by ATP-dependent contraction of the actomyosin cortex in permeabilized fibroblasts. J. Cell Sci. 98: 375–384
43. Deiss LP, Feinstein E, Berissi H, Cohen O and Kimchi A (1995) Identification of a novel serine/threonine kinase and a novel 15-kD protein as potential mediators of the gamma interferon-induced cell death. Genes Dev. 9: 15–30
44. Pato MD, Sellers JR, Preston YA, Harvey EV and Adelstein RS (1996) Baculovirus expression of chicken nonmuscle heavy meromyosin II-B. Characterization of alternatively spliced isoforms. J. Biol. Chem. 271: 2689–2695
45. Matsumura F, Ono S, Yamakita Y, Totsukawa G and Yamashiro S (1998) Specific localization of serine 19 phosphorylated myosin II during cell locomotion and mitosis of cultured cells. J. Cell Biol. 140: 119–129
46. Perrie WT and Perry SV (1970) An electrophoretic study of the low-molecular-weight components of myosin. Biochem. J. 119: 31–38